


# Design of cooperative matched filter for detection of chemical agents

Hyeong-Geun Yu Dr., Ph. D.,<sup>1</sup>  Chang Sik Lee Mr., M. S.,<sup>1</sup> Dong-Jo Park Prof., Ph. D.,<sup>1</sup> Dong Eui Chang Prof., Ph. D.,<sup>1,✉</sup> and Hyunwoo Nam Dr., Ph. D.<sup>2</sup>

<sup>1</sup>The School of Electrical Engineering, Korea Advanced Institute of Science and Technology, Daejeon, Republic of Korea

<sup>2</sup>The CRB Defense Technology Directorate, Agency for Defense Development, Daejeon, Republic of Korea

✉Email: dechang@kaist.ac.kr

A matched filter (MF) is one of the most widely used detectors for the detection of chemical agent (CA) clouds in the passive hyperspectral imaging system. To improve the detection performance of the MF, a linear cooperation scheme that allocates cooperation coefficients to the spectra of the neighbouring pixels is proposed. The optimal cooperation coefficients, which removes noise signatures whilst minimising the distortion of CA signatures, are acquired by finding the maximum likelihood estimator of the cooperation coefficients. It is proved that a moving average scheme that assigns the same coefficients is the optimal cooperation scheme. Finally, a cooperative MF with the optimal cooperation scheme is designed. It is demonstrated that the proposed cooperative MF is capable of robust detection performance via outdoor experiments with actual CA data measured by a Bruker HI-90 instrument.

**Introduction:** A Fourier transform infrared (FTIR)-based passive hyperspectral imaging system (HIS) becomes one of the key technologies for the detection of chemical agent (CA) clouds. The FTIR-based passive HIS sensor can measure the spectrum in each pixel for the instantaneous corresponding field of view at a standoff distance without an additional light source and can detect CA clouds in the atmosphere [1]. Many algorithms have been proposed to detect the CA signature by analysing spectra in the hyperspectral image (HSI) and to visualise the CA cloud [1–5]. Among the many detection algorithms developed thus far, the matched filter (MF) is considered to be a simple and powerful detection algorithm [2]. However, given the small light received at each pixel, the spectrum of each pixel has a low signal-to-noise ratio (SNR). As a result, the performance of these detection algorithms is limited.

In the HIS, the spectra of adjacent pixels have similar spectral data but different noise signatures. By combining spectra of neighbouring pixels, noise signatures in each spectrum can be reduced, and then the SNR can be improved. Several schemes that cooperate with spectra of neighbouring pixels have been proposed. There are two types of cooperation schemes, the hard and the soft cooperation schemes. The hard cooperation scheme, which merges the detection results of neighbouring pixels, is easy to implement [6]. The OR-rule, AND-rule, and majority rule belong to the hard cooperation scheme. But performance improvements are limited since each detection result is distorted by noise signatures in each pixel.

On the other hand, the soft cooperation scheme, which fuses the spectral data of neighbouring pixels, shows improved detection performance because it mitigates noise signatures in the spectra. The Gaussian filter (GF) and maximum noise fraction (MNF) are typical soft cooperation schemes [7, 8]. The GF is a soft cooperation scheme that assigns weights to spectra of neighbouring pixels according to the Euclidean distances between the centre and neighbouring pixels. The MNF is also a soft cooperation scheme, which reduces noise signatures by projecting the spectra into a less noisy subspace obtained using spectra of neighbouring pixels. However, given that these soft cooperation schemes only focus on removing the noise, they cause distortion of the CA signature. Therefore, it is necessary to retain the CA signature as well as minimise the noise signature.

In this study, we propose a linear cooperation scheme that assigns cooperation coefficients to neighbouring pixels. To optimise cooperation coefficients that minimise the noise signature whilst conserving the CA signature, we acquire the maximum likelihood estimator (MLE) of the cooperation coefficients. Then, we prove that the optimal linear cooperation

scheme is a moving average scheme, which allocates identical cooperation coefficients to the spectra of adjacent pixels. Finally, we design a cooperative MF. We conduct outdoor experiments with actual CA data measured by a Bruker HI-90 instrument. These experiments demonstrate the more accurate detection capabilities of the cooperative MF compared to those of other cooperation schemes.

**Conventional MF:** We briefly introduce the MF widely used for the remote detection of CA clouds. The FTIR-based passive HIS sensor measures light radiated from the background and that passes through the CA cloud and the atmosphere. Then, it generates HSI data with a spectral resolution of  $p$  channels and a spatial resolution of  $m \times n$  pixels. From the linear mixing model [1], the spectrum  $\mathbf{x} \in \mathbb{R}^p$  of a pixel in the measured HSI can be represented:

$$\begin{aligned} H_0 : \mathbf{x} &= \mathbf{v}, \\ H_1 : \mathbf{x} &= \mathbf{S}\mathbf{g} + \mathbf{v}. \end{aligned} \quad (1)$$

where  $H_0$  and  $H_1$  correspond to hypotheses stipulating the absence and presence of target CA clouds, respectively.

In Equation (1),  $\mathbf{S} = [\mathbf{s}_1, \dots, \mathbf{s}_{N_r}] \in \mathbb{R}^{p \times N_r}$  is the CA signature matrix, which consists of the CA signature vector  $\mathbf{s}_r \in \mathbb{R}^p$ , for  $r = 1, \dots, N_r$ . Here,  $N_r$  is the number of target CAs and  $p$  is the number of channels. In the experiment, the number of target CAs is set to seven,  $N_r = 7$ . The target CAs are sulfur hexafluoride ( $\text{SF}_6$ ), freon, tabun, sarin, mustard gas, methanol and triethyl phosphate. Each standard absorption spectrum of each target CA, which is established in the National Institute of Standard and Technology [11], is used as the target CA signature vector. The CA intensity vector is  $\mathbf{g} = [g_1, \dots, g_{N_r}]^T \in \mathbb{R}^{N_r}$ . The background clutter  $\mathbf{v} \in \mathbb{R}^p$ , which represents the summation of the background signature and noise follows a multivariate Gaussian distribution with mean  $\mathbf{m} \in \mathbb{R}^p$  and covariance  $\mathbf{C} \in \mathbb{R}^{p \times p}$ , i.e.,  $\mathbf{v} \sim N(\mathbf{m}, \mathbf{C})$ . Using the generalised likelihood ratio test (GLRT), the test statistic  $T_{MF}(\mathbf{x})$  of the MF is given as follows [2]:

$$T_{MF}(\mathbf{x}) = [(\mathbf{x} - \mathbf{m})^T \mathbf{C}^{-1} \mathbf{S}] [\mathbf{S}^T \mathbf{C}^{-1} \mathbf{S}]^{-1} [\mathbf{S}^T \mathbf{C}^{-1} (\mathbf{x} - \mathbf{m})]. \quad (2)$$

**Conventional matched filter:** We introduce a linear cooperation scheme that assigns cooperation coefficients to the spectra of neighbouring pixels. Let  $\mathbf{X} = [\mathbf{x}_1, \dots, \mathbf{x}_k] \in \mathbb{R}^{p \times k}$  be the cooperation spectrum set, which consists of the spectrum  $\mathbf{x}_1$  of the centre pixel and  $k - 1$  spectra of pixels adjacent to the centre pixel. Let  $\mathbf{X}\mathbf{a}$  represent a cooperation spectrum, which is a linear combination of the spectrum set  $\mathbf{X}$ . Here,  $\mathbf{a} = [a_1, \dots, a_k]^T \in \mathbb{R}^k$  is a cooperation coefficient vector. Because the spectra of adjacent pixels have similar spectral data in the HSI, we assume that if the spectrum  $\mathbf{x}_1$  is the CA spectrum, adjacent spectra are also CA spectra. Otherwise, they are all background spectra.

**Proposition 1.** *If the cooperation coefficient vector  $\mathbf{a}$  satisfies the equation  $a_1 + \dots + a_k = \mathbf{1}^T \mathbf{a} = 1$ , the cooperation spectrum  $\mathbf{X}\mathbf{a}|H_i$ , for  $i = 0, 1$  follows a Gaussian distribution as expressed below.*

$$\mathbf{X}\mathbf{a}|H_0 \sim N(\mathbf{m}, \mathbf{a}^T \mathbf{a} \mathbf{C}), \quad (3)$$

$$\mathbf{X}\mathbf{a}|H_1 \sim N(\mathbf{S}\mathbf{g} + \mathbf{m}, \mathbf{a}^T \mathbf{a} \mathbf{C}). \quad (4)$$

**Proof:** *Since the background clutter  $\mathbf{v}$  is a Gaussian random vector with mean  $\mathbf{m}$  and covariance  $\mathbf{C}$ , all spectra in  $\mathbf{X}$  are Gaussian random vectors with mean  $\mathbf{m}_i$ , for  $i = 0, 1$ , and covariance  $\mathbf{C}$ . Here,  $\mathbf{m}_0$  is  $\mathbf{m}$ , and  $\mathbf{m}_1$  is  $\mathbf{S}\mathbf{g} + \mathbf{m}$ . Then,  $\mathbf{X}\mathbf{a}$  follows a Gaussian distribution due to the central limit theorem. If  $\mathbf{a}$  satisfies  $a_1 + \dots + a_k = \mathbf{1}^T \mathbf{a} = 1$ , the mean vector  $\mathbf{m}_{\mathbf{X}\mathbf{a}|H_i}$  of  $\mathbf{X}\mathbf{a}|H_i$  is obtained as*

$$\mathbf{m}_{\mathbf{X}\mathbf{a}|H_i} = (a_1 + \dots + a_k)E(\mathbf{x}_k|H_i) = \mathbf{m}_i. \quad (5)$$

Assuming that each spectrum in  $\mathbf{X}$  is independent and identically distributed, the covariance matrix  $\mathbf{C}_{\mathbf{X}\mathbf{a}|H_i}$  of  $\mathbf{X}\mathbf{a}|H_i$  is also obtained as

$$\begin{aligned} \mathbf{C}_{\mathbf{X}\mathbf{a}|H_i} &= E(\mathbf{X}\mathbf{a} - \mathbf{m}_i|H_i)(\mathbf{X}\mathbf{a} - \mathbf{m}_i|H_i)^T \\ &= (a_1^2 + \dots + a_k^2) \mathbf{C} = \mathbf{a}^T \mathbf{a} \mathbf{C}. \end{aligned} \quad (6)$$

The likelihood function of  $\mathbf{Xa}$  under  $H_i$ , for  $i = 0, 1$  is represented as

$$P(\mathbf{Xa}|H_0) = \rho \exp \left[ -\frac{1}{2\mathbf{a}^T \mathbf{a}} (\mathbf{Xa} - \mathbf{m}_0)^T \mathbf{C}^{-1} (\mathbf{Xa} - \mathbf{m}_0) \right], \quad (7)$$

$$P(\mathbf{Xa}|H_1) = \rho \exp \left[ -\frac{1}{2\mathbf{a}^T \mathbf{a}} (\mathbf{Xa} - \mathbf{m}_1)^T \mathbf{C}^{-1} (\mathbf{Xa} - \mathbf{m}_1) \right],$$

where  $|\mathbf{C}|$  is the determinant of  $\mathbf{C}$  and  $\rho = \sqrt{1/(2\pi\mathbf{a}^T \mathbf{a})^p |\mathbf{C}|}$ .

*Cooperative matched filter:* The goal here is to find the optimal cooperation coefficient vector that mitigates the noise signature of the cooperation spectrum whilst minimising the distortion of CA signatures. Since the optimal cooperation coefficient vector maximises likelihood probability, we obtain the MLE, which maximises the likelihood probability  $P(\mathbf{Xa}|H_1)$  of the cooperation spectrum vector  $\mathbf{Xa}$  under  $H_1$ .

**Proposition 2.** *The optimal cooperation coefficient vector is  $\hat{\mathbf{a}} = 1/k$ .*

*Proof:* Define  $Q$  as the log-likelihood probability of the cooperation spectrum under  $H_1$ . We find the MLEs of  $\mathbf{g}$  and  $\mathbf{a}$ , which maximise  $Q$ . Given that the cooperation coefficient vector  $\mathbf{a}$  satisfies the equation  $\mathbf{1}^T \mathbf{a} = 1$ , we define the following optimisation problem as

$$\begin{aligned} \max_{\mathbf{g}, \mathbf{a}} Q &= \ln P(\mathbf{Xa}|H_1) \\ \text{subject to } &\mathbf{1}^T \mathbf{a} = 1. \end{aligned} \quad (8)$$

We can solve the Equation (8) using the Karush—Kuhn—Tucker conditions, which are necessary conditions for a solution to an optimisation problem [9].

First, we set the Lagrangian function for Equation (8) as follows:

$$\begin{aligned} L(\mathbf{g}, \mathbf{a}, \nu) &= -\frac{1}{2\mathbf{a}^T \mathbf{a}} (\mathbf{Xa} - \mathbf{Sg} - \mathbf{m})^T \mathbf{C}^{-1} (\mathbf{Xa} - \mathbf{Sg} - \mathbf{m}) \\ &\quad - \frac{\nu}{2} \ln(2\pi) - \frac{\nu}{2} \ln(\mathbf{a}^T \mathbf{a}) - \frac{1}{2} \ln|\mathbf{C}| - \nu(\mathbf{1}^T \mathbf{a} - 1), \end{aligned} \quad (9)$$

where  $\nu$  is a dual variable. Then, we obtain  $\hat{\nu}$ ,  $\hat{\mathbf{g}}$  and  $\hat{\mathbf{a}}$  satisfying  $\frac{\partial L}{\partial \mathbf{g}} = 0$ ,  $\frac{\partial L}{\partial \nu} = 0$ , and  $\frac{\partial L}{\partial \mathbf{a}} = 0$ . From  $\frac{\partial L}{\partial \mathbf{g}} = 0$ ,  $\hat{\mathbf{g}}$  is determined as

$$\hat{\mathbf{g}} = (\mathbf{S}^T \mathbf{C}^{-1} \mathbf{S})^{-1} \mathbf{S}^T \mathbf{C}^{-1} (\mathbf{Xa} - \mathbf{m}). \quad (10)$$

Next, the equation  $\mathbf{1}^T \mathbf{a} = 1$  is derived from  $\frac{\partial L}{\partial \nu} = 0$ .

Finally, we substitute  $\hat{\mathbf{g}}$  into  $\frac{\partial L}{\partial \mathbf{a}} = 0$  as follows:

$$\frac{\partial L}{\partial \mathbf{a}} = -\frac{\mathbf{a}}{(\mathbf{a}^T \mathbf{a})^2} \mathbf{m}^T \mathbf{A} (\mathbf{Xa} - \mathbf{m}) - \frac{p\mathbf{a}}{\mathbf{a}^T \mathbf{a}} - \nu \cdot \mathbf{1} = \mathbf{0}, \quad (11)$$

where  $\mathbf{A} = \mathbf{C}^{-1} - \mathbf{C}^{-1} \mathbf{S} (\mathbf{S}^T \mathbf{C}^{-1} \mathbf{S})^{-1} \mathbf{S}^T \mathbf{C}^{-1}$ . By multiplying  $\mathbf{a}^T$  by Equation (12), the optimal dual variable  $\hat{\nu}$  is determined as follows:

$$\hat{\nu} = \frac{\mathbf{m}^T \mathbf{A} \mathbf{m} - p\mathbf{a}^T \mathbf{a} - \mathbf{m}^T \mathbf{A} \mathbf{Xa}}{\mathbf{a}^T \mathbf{a}}. \quad (12)$$

By substituting  $\hat{\nu}$  into Equation (12), we acquire the following equation:

$$\frac{1}{\mathbf{a}^T \mathbf{a}} \left( \frac{\mathbf{a}}{\mathbf{a}^T \mathbf{a}} - \mathbf{1} \right) (\mathbf{m}^T \mathbf{A} \mathbf{m} - p\mathbf{a}^T \mathbf{a} - \mathbf{m}^T \mathbf{A} \mathbf{Xa}) = \mathbf{0}. \quad (13)$$

There are two solutions for Equation (13): Singular and regular solutions. The singular solution, which makes  $\hat{\nu} = 0$ , is a vector  $\mathbf{a}$  that satisfies both  $\mathbf{m}^T \mathbf{A} \mathbf{m} - p\mathbf{a}^T \mathbf{a} - \mathbf{m}^T \mathbf{A} \mathbf{Xa} = 0$  and  $\mathbf{1}^T \mathbf{a} = 1$ . However, the singular solution is the minimum solution for  $Q$ . The regular solution, which is a solution of  $\frac{\mathbf{a}}{\mathbf{a}^T \mathbf{a}} - \mathbf{1} = \mathbf{0}$ , is  $\mathbf{a} = 1/k$ . Given that the regular solution is the maximum solution for  $Q$ , the optimal cooperation coefficient vector  $\hat{\mathbf{a}}$  is  $1/k$ .

Proposition 2 implies that the optimal linear cooperation scheme is a moving average scheme, which allocates identical weights to all spectra in the cooperation spectrum set. At this point, we design the cooperative MF with the optimal cooperation scheme. Applying the GLRT to the

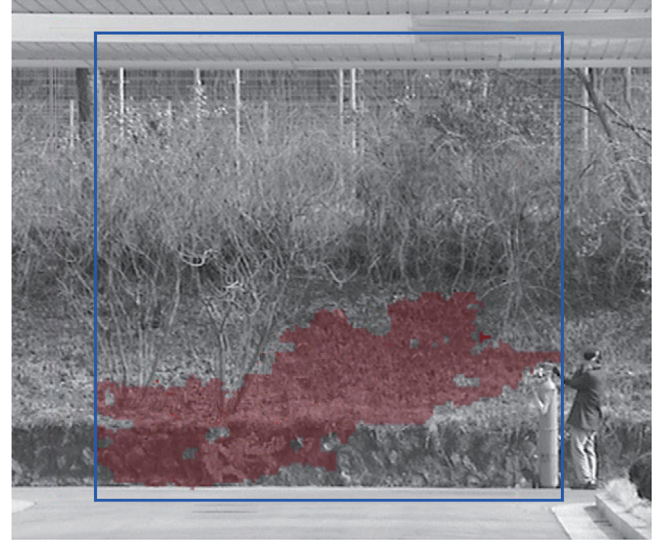


**Fig 1** Charge-coupled device image of hyperspectral image used in experiment

**Table 1.** Average log-likelihood probability,  $Q$

	Single	Gaussian filter	Maximum noise fraction	The proposed cooperation matched filter
$Q$	-409.51	-351.46	-336.60	-307.92

cooperation signal model, we derive the test statistic  $T_{CoMF}(\mathbf{X})$  of the cooperative MF as follows:

$$\begin{aligned} T_{CoMF}(\mathbf{X}) &= \frac{1}{k} [(\mathbf{X} \cdot \mathbf{1} - k\mathbf{m})^T \mathbf{C}^{-1} \mathbf{S}] [\mathbf{S}^T \mathbf{C}^{-1} \mathbf{S}]^{-1} \\ &\quad \cdot [\mathbf{S}^T \mathbf{C}^{-1} (\mathbf{X} \cdot \mathbf{1} - k\mathbf{m})]. \end{aligned} \quad (14)$$

If  $T_{CoMF}(\mathbf{X})$  exceeds the detection threshold  $\lambda$ , the pixel corresponding to the centre spectrum  $\mathbf{x}_1$  in the cooperation spectrum set is classified as a CA cloud pixel. Otherwise it is determined as a background pixel.

*Experimental results:* We describe the experiments conducted to compare the proposed cooperation scheme with other cooperation schemes on real HSI data measured by an HI-90 equipment manufactured by the Bruker Corporation. The HI-90 equipment provides HSI data with a spectral resolution of  $3.2 \text{ cm}^{-1}$  from  $903 \text{ cm}^{-1}$  to  $1264 \text{ cm}^{-1}$  with 128 channels and a spatial resolution of  $128 \times 128$  pixels [10]. The experimental scenario is one in which the  $\text{SF}_6$  gas was sprayed into the air with a grass field as the background. Figure 1 shows the charge-coupled device image of the HSI used in the experiment. The blue box shows the area of the HSI, and the red pixels represent the area in which the  $\text{SF}_6$  cloud exists. The  $\text{SF}_6$  gas area was obtained by applying several detection algorithms [1–5] to the HSI and eliminating some outlier pixels. The background statistics, that is, mean  $\mathbf{m}$  and covariance  $\mathbf{C}$ , are calculated from the HSI data measured before the spraying of the  $\text{SF}_6$  gas.

To evaluate how noise signatures are removed whilst minimising distortion of CA signatures, we obtain the average log-likelihood probabilities  $Q$  for the cooperation spectra of the  $\text{SF}_6$  pixels according to several cooperation schemes as shown in Table 1. There are four cooperation schemes: A non-cooperation scheme (single), a GF, an MNF and the proposed cooperation scheme. When all cooperation schemes are applied, a  $3 \times 3$  window, which maximises the effect of cooperation schemes, is used. The single represents a non-cooperation scheme.

As shown in Table 1, the log-likelihood probabilities of the GF and MNF are higher than that of the non-cooperation scheme because the GF and MNF suppress noise signatures. The proposed cooperation scheme has the highest log-likelihood probability since it minimises the distortion of the  $\text{SF}_6$  signature. To compare the detection performances of the MFs with several cooperation schemes applied, we present images of the test statistics of the MFs with these schemes in Figure 2. The

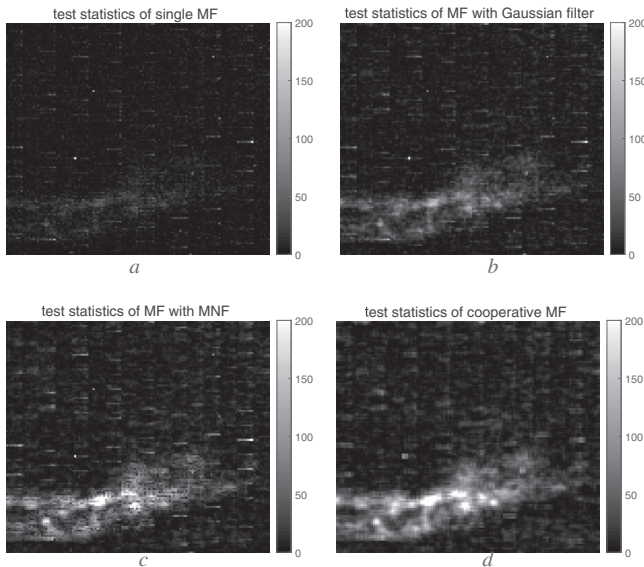


**Fig 2** Images of test statistics. (a) Single matched filter (MF), (b) MF with Gaussian filter, (c) MF with maximum noise fraction, (d) the proposed cooperative MF

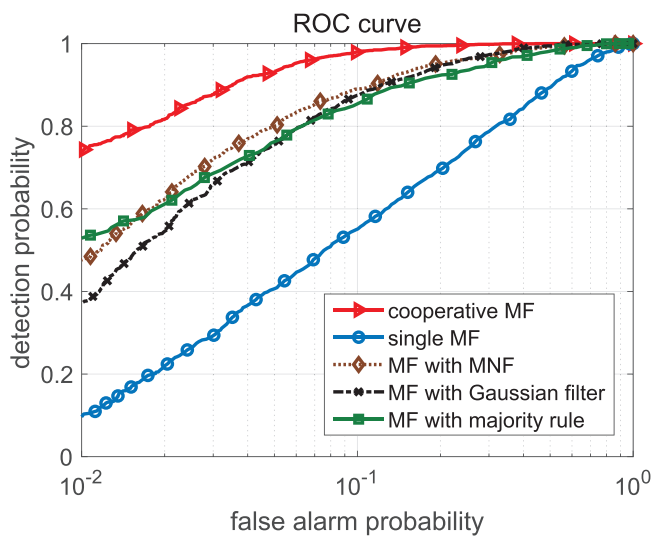


**Fig 3** Receiver operating characteristic curves of MFs with several cooperation schemes

accurate detection algorithm results in a greater difference between the test statistics of the background pixels and those of the SF<sub>6</sub> pixels. As shown in Figure 2(a), there is a slight difference between the test statistics of the background and the SF<sub>6</sub> pixels because the test statistics of the SF<sub>6</sub> pixels are not increased due to noise signatures. As shown in Figures 2(b)–(d), the test statistics of the SF<sub>6</sub> spectra are increased considerably.

For a more objective-detection performance comparison, we obtain the receiver operating characteristic curves of the MFs with several cooperation schemes as shown in Figure 3. The majority rule is a hard cooperation scheme that gathers the detection results for all spectra in the  $3 \times 3$  window and determines whether the centre spectrum is the SF<sub>6</sub> cloud spectrum or the background spectrum according to a majority vote. As shown in Figure 3, the single MF shows poor detection performance. The majority rule performs as well as the MNF. The detection performance of the proposed cooperative MF is better than those of the other schemes, which is in agreement with the results from the test statistics images shown in Figure 2. The experimental results confirm that the proposed cooperative MF improves the detection performance by mitigating noise signatures whilst preserving SF<sub>6</sub> signatures.

**Conclusion:** To improve an MF, which is one of the most popular algorithms for detecting CA clouds, we proposed a linear cooperation scheme that integrates the spectral data of neighbouring pixels. In the proposed cooperation scheme, the optimal cooperation coefficient vector, which mitigates the noise signature and minimises the distortion of the CA signature, was computed by maximising the log-likelihood probability. It is proved that the optimal cooperation scheme is a moving average scheme, which allocates the identical cooperation coefficients. Finally, we designed the cooperative MF using the optimal cooperation scheme. The experimental result confirmed that the cooperative MF has better detection performance than other cooperation schemes. The cooperative MF can be widely adopted in various detection fields in which conventional MFs can be applied. The future research is to study schemes tracking CA clouds in sequentially measured HSIs for which more complex cooperation schemes considering a time-varying condition like in [12, 13].

**Acknowledgements:** This work has been supported by Agency for Defense Development of the Republic of Korea and Brain Korea 21 program.

© 2021 The Authors. *Electronics Letters* published by John Wiley & Sons Ltd on behalf of The Institution of Engineering and Technology

This is an open access article under the terms of the Creative Commons Attribution License, which permits use, distribution and reproduction in any medium, provided the original work is properly cited.

Received: 10 October 2020 Accepted: 6 January 2021

doi: 10.1049/ell2.12088

## References

- Manolakis, D., Golowich, S. E., DiPietro, R. S.: Long-wave infrared hyperspectral remote sensing of chemical clouds: A focus on signal processing approaches. *IEEE Signal Process Mag.* **31**(4), 120–141 (2014)
- Truslow, E., et al.: Performance prediction of matched filter and adaptive cosine estimator hyperspectral target detectors. *IEEE J. Sel. Top. Appl. Earth Obs. Remote Sens.* **7**, 2337–2350 (2014)
- Wang, Y., Chen, G., Maggioni, M.: High-dimensional data modeling techniques for detection of chemical plumes and anomalies in hyperspectral images and movies. *IEEE J. Sel. Top. Appl. Earth Obs. Remote Sens.* **9**(9), 4316–4324 (2016)
- Harig, R., Matz, G.: Toxic cloud imaging by infrared spectrometry: a scanning FTIR system for identification and visualization. *Field Anal. Chem. Technol.* **5**(1–2), 75–90 (2001)
- Nam, H., et al.: Development of a radiative transfer model for the determination of toxic gases by Fourier transform-infrared spectroscopy with a support vector machine algorithm. *Instrum. Sci. Technol.* **47**, 1–14 (2018)
- Benediktsson, J. A., Kanellopoulos, I.: Classification of multisource and hyperspectral data based on decision fusion. *IEEE Trans. Geosci. Remote Sens.* **37**(3), 1367–1377 (1999)
- Alam, M. S., et al.: Hyperspectral target detection using gaussian filter and post-processing. *Opt. Lasers Eng.* **46**(11), 817–822 (2008)
- H.-G. Yu, et al.: Noise reduction for improving the performance of gas detection algorithms in the FTIR spectrometer. *Proc. SPIE* **10433**, 106441Q (2018).
- Chong, E. K. P., Zak, S. H.: *An Introduction to Optimization* (4th edition). John Wiley & Sons, New York (2013)
- Sabbah, S., et al.: Remote sensing of gases by hyperspectral imaging: System performance and measurements. *Opt. Eng.* **51**(11), 1117179 (2012)
- Chu, P. M., et al.: The NIST quantitative infrared database. *J. Res. Nat. Inst. Stand. Technol.* **104**(1), 59–81 (1999)
- Sundaresan, A., Varshney, P. K., Rao, N. S.: Distributed detection of a nuclear radioactive source based on a hierarchical source model. In: 2009 IEEE International Conference on Acoustics, Speech and Signal Processing, Taipei, Taiwan, pp. 2901–2904 (2009) doi: 10.1109/ICASSP.2009.4960230
- Ciunzo, D., et al.: Distributed classification of multiple moving targets with binary wireless sensor networks. In: IEEE 14th International Conference on Information Fusion, Chicago, Illinois, pp. 1–8 (2011) <https://ieeexplore.ieee.org/abstract/document/59775>